Time-Resolved Fluorescence and Small Angle Neutron Scattering Study in Pluronics−Surfactant Supramolecular Assemblies

Prabhat K. Singh,[†] Manoj Kumbhakar,[†] Rajib Ganguly,[‡] Vinod K. Aswal,[¶] Haridas Pal,[†] and Sukhendu Nath*[,†]

Radiation & Photochemistry Division, Chemistry Division, and Solid State Physics Division, Bhabha Atomic Research Centre, Mumbai 400 085, India

Received: September 29, 2009; Revised Manuscript Received: January 29, 2010

Interaction of cationic surfactant, cetyl trimethyl ammonium bromide (CTAB), with pluronics F88 ($EO_{103}-PO_{39}-EO_{103}$) and P105 ($EO_{37}-PO_{56}-EO_{37}$) micelles and its effect on modulating the location of an anionic solute in the mixed micelles have been investigated using time-resolved fluorescence and small angle neutron scattering (SANS) studies. SANS results indicate the formation of pluronic−CTAB supramolecular assemblies, in which the hydrophobic chains of CTAB occupy the hydrophobic core of the pluronic micelle while the positively charged head groups reside at the micellar core−corona interface. Rotational correlation time of the anionic probe in these supramolecular assemblies increases with an increase in the CTAB concentration, and the observed results are explained on the basis of the probe movement from the surface to the interior of the micelle due to the increased electrostatic attraction. Dynamic Stokes' shift measurements also support the movement of the probe due to the addition of the surfactant to the supramolecular assemblies. From the studies with different pluronics, it is indicated that the concentration of CTAB required to drag the probe molecule into the interior of the micelles is linearly correlated to the thickness of the corona region of the respective micelles.

1. Introduction

Pluronics, the triblock copolymers, made up of poly(ethyleneoxide) (EO) and poly(propyleneoxide) (PO) blocks, with general formula $(EO)_n-(PO)_m-(EO)_n$, have been the subject of intense research over last two decades due to their unique solution behavior[1–6] and extensive industrial applications.[7,8] Use of these pluronics as drug encapsulation and drug delivery systems has been well-demonstrated.[9–13] They also have promising use in the synthesis of different nanostructures.[14–18] Pluronics form micelles in aqueous solution above a certain concentration, known as the critical micellar concentration (CMC).[2,3,6] Pluronic micelles are known to form a core−shell structure with the PO block forming the hydrophobic core, which is surrounded by the relatively hydrophilic EO blocks, known as the corona region.

In several industrial applications, pluronics are used in combination with other surfactants.[19,20] The presence of two different classes of surfactants results in the formation of complex microheterogeneous systems. For efficient use of such complex microheterogeneous systems, it is required that their properties be understood in detail. In most of the applications of these microheterogeneous media, a solute is dissolved in the micelle, and its efficiency for a specific process largely depends on its physical and chemical properties inside the micellar phase. Because the microheterogeneous media can provide a wide range of microenvironments, the physical and chemical properties of a dissolved solute can be modulated significantly, depending on its location in the microheterogeneous media. Thus, it is important to find out a suitable methodology to tune the location of the dissolved solute in the microheterogeneous media for possible modification of the physical and chemical properties of these solutes for their suitable applications.

It is reported that some pluronics form unique supramolecular assemblies in the presence of ionic surfactants (e.g. sodium dodecyl sulfate (SDS)),[21–25] where the hydrophobic chain of the surfactant gets dissolved in the core of the pluronic micelle and the charged headgroup resides at the peripheral region of the core projecting into the hydrated corona region. Because of this unique structure, a charged layer is formed inside the mixed micelle, which can attract an oppositely charged solute from the micellar surface to its interior. In the present study, we have investigated the pluronic F88 ($EO_{103}-PO_{39}-EO_{103}$) and P105 ($EO_{37}-PO_{56}-EO_{37}$) in the presence of cetyl trimethyl ammonium bromide (CTAB) to understand the structures of the mixed micellar systems and also to see if the position of a dissolved solute can be modulated by changing the composition of the these mixed micellar systems. The results in F88−CTAB and P105−CTAB systems have also been compared with those of other pluronic−surfactant systems reported earlier to understand the effect of block size on the observed behavior of such supramolecular assemblies.

2. Methods and Materials

Steady-state absorption and fluorescence spectra were measured using a Shimadzu spectrophotometer (model UV-160A) and a Hitachi spectrofluorometer (model 4010F), respectively. Time-resolved fluorescences were measured using a time-correlated single-photon-counting instrument from IBH (U.K.). Sample was excited with a 408 nm diode laser, and emission was detected using a PMT-based detector. The instrument response function for the present setup is 230 ps (full width at

* Corresponding author. Phone: 91-22-25590306. Fax: 91-22-5505151. E-mail: snath@barc.gov.in.
[†] Radiation & Photochemistry Division.
[‡] Chemistry Division.
[¶] Solid State Physics Division.

10.1021/jp909333q
Published on Web 02/26/2010

SCHEME 1: Molecular Structures of Chemicals Used in the Present Study

$HO(-CH_2-CH_2-O-)_{103}(-CHMe-CH_2-O-)_{39}(-CH_2-CH_2-O-)_{103}H$

F88

$HO(-CH_2-CH_2-O-)_{37}(-CHMe-CH_2-O-)_{56}(-CH_2-CH_2-O-)_{37}H$

P105

$CH_3-(CH_2)_{15}-N^+(CH_3)_3Br^-$

CTAB

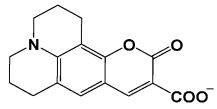

C343 anion

half maximum). All optical measurements were carried out in a quartz cell with 1 cm optical path length.

Time-dependent anisotropy was calculated using the following equation,[26]

$$r(t) = \frac{I_{||}(t) - GI_{\perp}(t)}{I_{||}(t) + 2GI_{\perp}(t)} \quad (1)$$

where $I_{||}(t)$ and $I_{\perp}(t)$ are measured fluorescence decays for the parallel and perpendicular polarizations with respect to the vertically polarized excitation beam. The factor G is the correction factor for the polarization sensitivity of the detection system and was estimated independently.[26] All these measurements were carried out two to three times to check the reproducibility and to obtain the average values for the rotational relaxation times.

Neutron scattering measurements were carried out using the facility at the Dhruva reactor, Trombay, India. The mean incident wavelength (λ) of the neutron was 5.2 Å with $\Delta\lambda/\lambda = 15\%$. The scattered neutrons were measured for the scattering vector (q) range of 0.02−0.3 $Å^{-1}$. The measured SANS data were corrected for the background, the empty cell contribution, and the transmission and were presented on an absolute scale using the standard protocols.[27] Correction due to the instrumental smearing was also taken into account throughout the data analysis.[27] All SANS measurements were carried out in D_2O media.

F88 was a gift from BASF corporation, Edison, NJ. CTAB (Aldrich), SDS (Fluka), P105 (Aldrich), and Coumarin 343 (C343, Exciton) were used as received. F88 solution of 5% w/v was prepared in nanopure water (with conductivity less than 0.1 $\mu S\ cm^{-1}$) obtained from a Millipore Milli Q system. The concentration of C343 in the experimental solution was kept very low (∼1−2 μM) so that the possibility of having more than one dye in a micelle is negligible. It was shown earlier that the critical micellar temperature (CMT) for 5% w/v F88 is ∼35 °C,[28–30] and thus, all the experiments with F88 were carried out at 40 °C to ensure complete micellization. Similarly, all experiments with P105 (CMT for 5% w/v is 20.3 °C[31]) were carried out at 30 °C to ensure the complete micellization of the polymer. Molecular structures of the chemicals used in the present study are given in Scheme 1.

3. Results and Discussions

3A. F88−CTAC. ***3A.1. Steady-State Absorption and Fluorescence Studies.*** Depending on the solution pH, the probe, coumarin 343 (C343), can exist in different prototropic forms in water. To find out the actual prototropic form of the dye present in the micellar solution, the absorption spectra of C343 in F88 solution were measured at different pHs. The neutral and anionic forms of C343 are known to have quite different absorption spectra, with their absorption maxima at 450 and 425 nm, respectively.[32] Figure 1 shows the changes in the absorbance for C343 dye in F88 micellar solution measured at 450 nm with the change in the pH of the solution. The decrease in the absorbance at 450 nm with increasing pH is due to the conversion of neutral C343 to anionic C343. The pK_a value for C343 in F88 micellar solution is thus estimated to be 5.4. It is to be mentioned that the pK_a value for C343 in water is reported to be 4.6.[32] An upward shift in the pK_a value of a solute in a micellar solution as compared with that in bulk water is well-documented in the literature and is believed to be due to the changes in the water structure around the solute in these two media.[33] It is also reported in the literature that the presence of an ionic surfactant can induce a further change in the pK_a value of a solute due to the possible Coulombic interaction with different prototropic forms of the solute. The cationic surfactant, such as CTAB used in the present study, is known to lower the pK_a value of a solute dissolved in the micellar media.[33] Thus, because of the decrease in the pK_a value in the presence of cationic surfactant, the nature of the prototropic form of C343 in F88 micellar solution should not change due to the addition of CTAB if the pH of the solution is kept significantly higher than 5.4. In the present study, the pH of the F88 solution used for all optical and SANS studies was kept about 7.2. Thus, we assume that C343 exists exclusively in its anionic form in all experimental solutions, even in the presence of CTAB. The presence of the anionic form of C343 in different pluronic micelles[28,29,34,35] and other reverse micelles[32,36,37] has, in fact, been reported in the literature.

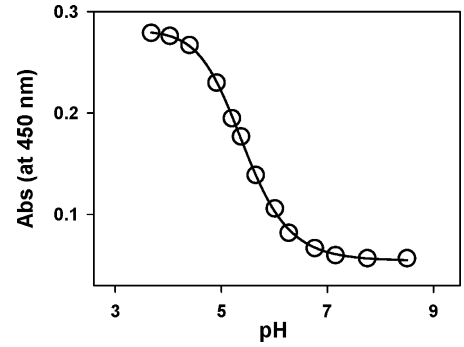

Figure 1. Changes in absorbance of the C343 dye (at 450 nm) with pH of the 5% w/v F88 solution.

Steady-state emission spectra of C343 in F88 micellar solution were recorded at different CTAB concentrations to understand the possible changes in the microenvironment for the probe due to the addition of CTAB. Observed results, as shown in Figure 2, indicate that with an increase in the CTAB concentration, the emission spectra of C343 gradually shift toward the shorter wavelength. Such a hypsochromic shift in the emission spectra suggests that the polarity of the microenvironment around the probe decreases gradually on increasing the CTAB concentration in the F88 micellar solution.

3A.2. Time-Resolved Fluorescence Anisotropy Studies. To understand more about the changes in the microenvironment of the dye with the added CTAB in the F88 micellar solution, we have further carried out the time-resolved fluorescence anisotropy measurements in the present system. The changes in the anisotropy decay for C343 in F88 solution at different CTAB concentrations are shown in Figure 3A. For comparison, the anisotropy decay for C343 in bulk water, which is very fast compared to those in F88−CTAB solutions, is also shown in

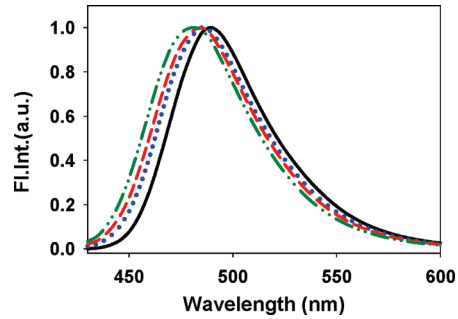

Figure 2. Steady-state emission spectra of C343 in 5% w/v F88 solution at different CTAB/F88 molar ratios: 0.0 (—) 0.1 (••••), 0.2 (– – –) and 0.5 (—••—••—).

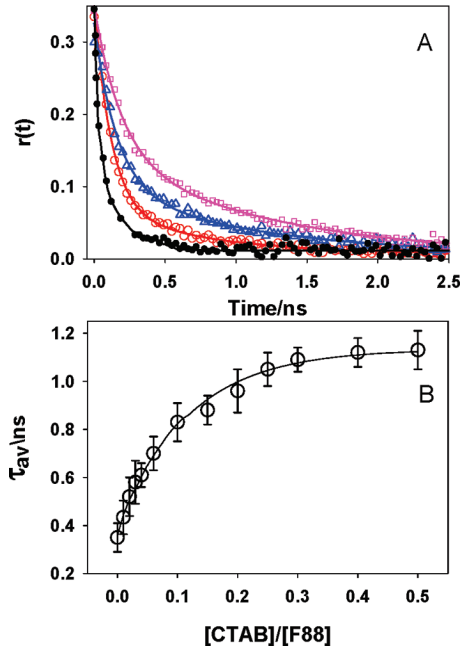

Figure 3. (A) Fluorescence anisotropy decay for C343 dye in water (●) and in F88 micellar solution at different CTAB/F88 molar ratios: (○) 0.0, (△) 0.1, and (□) 0.3. (B) Variation of the average reorientation time for C343 dye in F88 micellar solution with the CTAB/F88 molar ratio.

Figure 3A. The observation that the anisotropy decay for the dye in F88 solution is much slower than that in the bulk water suggests that C343 preferentially resides in the micellar phase. Because of the ionic nature, although a small fraction of the dye might be partitioned in the bulk water, this fraction is expected to be much less as compared to that in the micellar phase because the dye C343 possess a large hydrophobic group in its structure.[28,29,34] However, since the probe is ionic in nature, it is expected to reside preferentially at the micellar surface rather than entering deep into the micelle under normal circumstances.[28,29,34]

As indicated from Figure 3A, the anisotropy decay gradually becomes slower as the CTAB concentration is increased in the F88 solution. The anisotropy decays for the present systems were fitted with a biexponential function, as given by the following equation,

$$r(t) = \sum_{i=1}^{2} a_{ri} \exp(-t/\tau_{ri}) \qquad (2)$$

where a_{ri} and τ_{ri} are the amplitude and time constant, respectively, for the ith decay component. The biexponential nature of the anisotropy decay for a fluorophore in micellar media is well-documented[38–42] and has been explained on the basis of the wobbling-in-cone motion of the probe inside the micelle.[43] The average rotational relaxation time, τ_{av}, was calculated using the following equation,[26]

$$\tau_{av} = a_1\tau_{r1} + a_2\tau_{r2} \qquad (3)$$

where

$$a_i = a_{ri}\tau_{ri} / \sum_{i=1}^{2} a_{ri}\tau_{ri}$$

All the fitting parameters, including the τ_{av} values for C343 dye in F88 micellar solution at different CTAB concentrations, are listed in Table 1. The error limits in the τ_{av} values were obtained from multiple measurements. The variation in the τ_{av} values with the CTAB concentration is shown in Figure 3B. The τ_{av} initially increases and then saturates to a limiting value at a CTAB/F88 molar ratio of about 0.4. The increase in the rotational reorientation time with the increase in the CTAB concentration clearly indicates that the probe gradually experiences more frictional force in the micellar media with the increase in the CTAB concentration. Present observation suggests that the microviscosity around the probe in the F88 micelle increases with an increase in the CTAB concentration.

TABLE 1: Time-Resolved Anisotropy Parameters with Varying [CTAB]/[F88] Molar Ratios

CTAB/F88 molar ratio	τ_{r1} (ns)	a_1	τ_{r2} (ns)	a_2	τ_{av} (ns)
0.00	0.15	0.38	0.48	0.62	0.35 ± 0.06
0.01	0.07	0.30	0.74	0.70	0.43 ± 0.07
0.02	0.08	0.30	0.77	0.70	0.52 ± 0.08
0.03	0.08	0.29	0.78	0.71	0.58 ± 0.09
0.04	0.08	0.29	0.82	0.71	0.61 ± 0.05
0.06	0.07	0.22	0.88	0.78	0.70 ± 0.07
0.10	0.09	0.21	1.03	0.79	0.83 ± 0.08
0.15	0.09	0.15	1.02	0.85	0.88 ± 0.06
0.20	0.09	0.15	1.12	0.85	0.96 ± 0.09
0.25	0.12	0.15	1.22	0.85	1.05 ± 0.07
0.30	0.12	0.13	1.23	0.87	1.09 ± 0.05
0.40	0.14	0.13	1.27	0.87	1.12 ± 0.06
0.50	0.17	0.14	1.29	0.86	1.13 ± 0.08

3A.3. Small Angle Neutron Scattering (SANS) Studies. To understand more about the nature of the interaction between F88 and CTAB in the present supramolecular assemblies, we have also carried out SANS studies using 5% w/v F88 solution (in D_2O) in the absence and presence of CTAB. The differential scattering cross section per unit volume ($d\Sigma/d\Omega$) of a monodisperse micelle can be expressed as[44]

$$d\Sigma/d\Omega = NF_{mic}(q)\,S(q) + B \qquad (4)$$

where N is the number density of the micelles, and B is a constant representing the incoherent background scattering mainly from the hydrogen atoms present in the sample. $F_{mic}(q)$ is the form factor, characteristic of the size and the shape of the scatterers, and $S(q)$ is the structure factor that accounts for the interparticle interaction. Structurally, the pluronic micelles can be considered as the core−shell particles with different scattering length densities for the PPO core and the PEO shell.[45,46] In the present SANS analysis, $F_{mic}(q)$ was considered

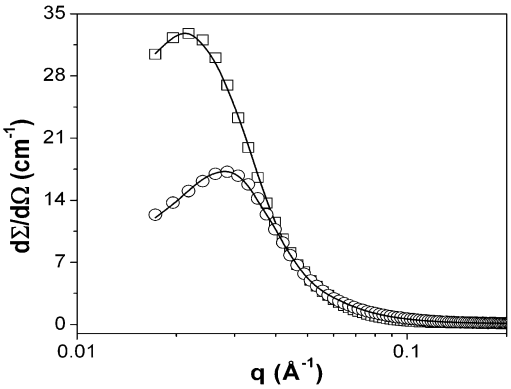

Figure 4. SANS data of the F88 solutions at different CTAB/F88 molar ratios (0 (□) and 0.5 (○)). The solid lines are fit to the data using a mixed micellar model as discussed in the text.

for a spherical micelle, as formulated by Pedersen,[45] and it depends on the radius of the hydrophobic micellar core. The analytical form of the $S(q)$ factor for the block copolymer micelles was obtained from the analytical solution of the Ornstein−Zernike equation in the Percus−Yevick approximation, employing the hard sphere potential.[47] It is shown in the literature that the $S(q)$ factor is a function of the hard sphere radius (R_{hs}), and the micellar volume fraction ϕ, which is defined as[48–50]

$$\phi = \frac{C4\pi R_{hs}^3}{3N_{agg}} \tag{5}$$

where C is the concentration of the pluronic in w/v % and N_{agg} is the aggregation number, which can be determined from the knowledge of the core size.[51]

For polydisperse micelles, eq 4 can be written as

$$\frac{d\Sigma}{d\Omega}(q) = \int \frac{d\Sigma}{d\Omega}(q,R)\, f(R)\, dR + B \tag{6}$$

In the present study, the polydispersity in the micellar size (R_c) was accounted for by the Schultz distribution, as given by the following equation,[52]

$$f(R_c) = \left(\frac{z+1}{R_{cm}}\right)^{z+1} R_c^z \exp\left[-\left(\frac{z+1}{R_{cm}}\right)R_c\right]\frac{1}{\Gamma(z+1)} \tag{7}$$

where Γ is the gamma function, R_{cm} is the mean core radius of the micelles, and the parameter z is a function of the width (ΔR_c) of core radius, defined by the following equation,

$$z = (R_{cm}/\Delta R_C)^2 - 1 \tag{8}$$

The mean core radius, the polydispersity for the core radius ($\Delta R_c/R_{cm}$), the micellar volume fraction (ϕ), and the hard sphere radius of the micelles are the fitting parameters in the analysis of the SANS data.

Figure 4 shows the SANS patterns for 5% w/v F88 solutions at two different CTAB concentrations. As reported in the case of the SDS−pluronic system,[23] in the present case also, the addition of CTAB leads to a decrease in the scattering cross section and a shift in the peak position to a higher q value. Recent NMR and SANS studies on mixed pluronic−ionic surfactant systems suggest that the hydrophobic chain of ionic surfactants are dissolved in the hydrophobic core of the pluronic micelles to avoid unfavorable interaction with the water molecules.[23,53] On the basis of this report, we have analyzed our SANS data assuming that the hydrophobic chains of CTAB also get dissolved in the hydrophobic core of the F88 micelles and the charged head groups reside at the interface of the core and corona region, as reported for the P123−SDS system.[23] This consideration gave us a good fit to the experimental SANS data, suggesting the absence of any second type of aggregates in the form of pure CTAB micelles. The solid lines in Figure 4 represent the fitted data according to the above mixed micellar model. Parameters obtained from the fit to the experimental data are summarized in Table 2. It is seen from Table 2 that as in the case of other surfactant−copolymer systems, the R_{cm} decreases with an increase in the CTAB concentration due to an increase in the hydrophilic character of the micellar system in the presence of the ionic surfactants. The micellar volume fraction remains effectively unchanged with the increase in the CTAB concentration. Thus, the SANS results clearly support the formation of a supramolecular structure due to the addition of CTAB to F88 micellar solution.

In the light of the results obtained from the SANS study, the changes in the photophysical properties and in the rotational correlation times of the probe, C343 anion, can be explained from the following consideration. As we add CTAB to the F88 micellar solution, it forms a supramolecular assembly such that the hydrophobic long chain of the CTAB molecule gets dissolved in the core of the F88 micelle. The charged headgroup of the CTAB molecule, however, resides at the interface of the core and corona region of the micelle. Due to the formation of such supramolecular assemblies, a positively charged layer is developed inside the F88 micelle in the presence of CTAB. The charge density of this layer in the F88 micelle increases gradually as we increase the CTAB concentration.

Because the probe used in the present study is anionic in nature, it experiences an electrostatic attraction by the positively charged layer developed in the F88 micelle due to the presence of CTAB. This electrostatic attraction leads to a gradual movement of the anionic probe from the surface of the micelle to its interior region as we increase the CTAB concentration. Thus, the increase in the reorientation time of the probe with an increase in the CTAB concentration in F88 micelle is attributed to the following two reasons: First, the microviscosity of the interior of the micelle is much higher than that at the micellar surface. Second, the increase in the electrostatic interaction between the negatively charged probe and the positively charged layer inside the micelle acts against the rotational motion of the probe. Thus, there is a gradual increase in the τ_{av} values of the dye in the F88 micelle with an increase in the CTAB concentration.

The probe movement from the micellar surface to its interior is also responsible for the observed hypsochromic shift in its emission spectra with the addition of CTAB (cf. Figure 2). The surface of the micelle is exposed to the bulk water and, thus, has a higher dielectric constant as compared to that in the interior of the micelle. A decrease in the dielectric constant of the microenvironment due to the change in the location of the probe results in the observed changes in the photophysical properties.

The SANS study indicates that there are, in fact, some changes in the micellar characteristics due to the addition of CTAB to the F88 micellar solution. To check whether these

TABLE 2: The Core Radius, the Hard Sphere Radius, the Volume Fraction, and the Polydispersity of the Micelles in 5% w/vF88 Solutions with Different CTAB Concentrations[a]

CTAB/F88 molar ratio	core radius, R_{cm} (nm)	hard sphere radius, R_{hs} (nm)	volume fraction, ϕ	polydispersity, $\Delta R_c/R_{cm}$ (%)
0.0	3.26 ± 0.02	11.7 ± 0.1	0.23 ± 0.01	25 ± 0.1
0.5	2.58 ± 0.02	9.8 ± 0.2	0.26 ± 0.02	27 ± 0.1

[a] The scattering length densities used to fit the data are 0.603 × 10^{10} cm^{-2}, 0.343603 × 10^{10} cm^{-2} and 6.38603 × 10^{10} cm^{-2} for EO, PO and D_2O, respectively.[64]

changes in the micellar characteristics have any effect on the rotational motion of the probe, we have also measured the reorientation time of a cationic dye, Rhodamine-110 (R110), in the F88 micellar solution at different CTAB concentrations. It is reported that, like C343, R110 also resides preferentially at the surface of the pluronic micelles.[54] The average reorientation time for R110 in the F88 at CTAB/F88 molar ratios of 0 and 0.5 is found to be effectively the same, ~0.34 ns. This reorientation time for R110 is also very similar to that observed for the C343 dye in the F88 solution in the absence of CTAB (cf. Table 1). These results indicate that the microenvironment of C343 and R110 are very similar in an F88 micellar solution in the absence of CTAB. Similar reorientation time for R110 in F88 micellar solution at different CTAB concentrations clearly indicates that the dye always resides at the micellar surface and the small changes in the F88 micellar characteristics due to the addition of CTAB do not change the reorientation time of the probe that resides at the micellar surface. Because R110 is a positively charged dye, there will be no electrostatic attraction between CTAB and R110. Thus, there is no effective movement of R110 in the F88 micelle due to the formation of the supramolecular structure by the addition of CTAB in the F88 solution. Thus, the observed changes in the reorientation times for anionic C343 dye with the CTAB concentration in the F88 micellar solution must not be due to the changes in the micellar characteristics, but certainly due to the changes in the location of the probe in the micellar phase.

3B. P105−CTAB. ***3B.1. Time-Resolved Fluorescence Anisotropy Studies.*** If there is a movement of the solute molecule from the micellar surface to its interior due to the electrostatic attraction, it is expected that the location of the solute in the micellar phase can also be controlled by controlling the thickness of the corona region. For example, in micelles with a thicker corona region, the spatial separation between the probe at the surface and the charged layer at the core−corona interface will be large and subsequently should need a higher surfactant concentration to pull the probe from the surface, in comparison to that with thinner corona region. To check this possibility, we have also carried out the time-resolved anisotropy measurement with another pluronic (namely, P105) which has a relatively thin corona region (31 Å[55]) as compared to that of F88 micelle (46 Å[51]). Figure 5A shows the variation of the fluorescence anisotropy with time for C343 in the P105−CTAB system with different CTAB/P105 molar ratios. Similar to the case of F88−CTAB, in the P105−CTAB system, it is also seen that the anisotropy decay becomes slower with an increase in the CTAB concentration. The variation in the average reorientation time,τ_{av}, of the C343 dye in the P105−CTAB system with the surfactant concentration is listed in Table 3 and presented in Figure 5B. It is evident from Figure 5B that as in the F88−CTAB system, in the P105−CTAB system, the reorientation time also increases with the CTAB concentration and reaches saturation at a CTAB/P105 molar ratio of ~0.3. However, the value of the CTAB/F88 molar ratio required to attain a similar saturation in the reorientation time is seen to be ~0.4 (cf. Figure 3B), higher than that required in the case of

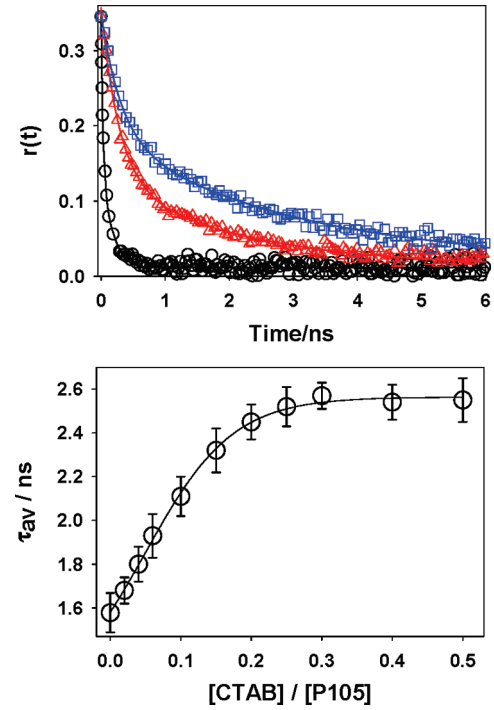

Figure 5. (A) Fluorescence anisotropy decay for C343 dye in water (○) and in the P105 micellar solution at different CTAB/P105 molar ratios: (△) 0.0 and (□) 0.25. (B) Variation of the average reorientation time for the C343 dye in the P105 micellar solution vs the CTAB/P105 molar ratio.

TABLE 3: Time-Resolved Anisotropy Parameters with Varying [CTAB]/[P105] Molar Ratios

CTAB/P105 molar ratio	τ_{r1} (ns)	a_1	τ_{r2} (ns)	a_2	τ_{av} (ns)
0	0.32	0.26	2.02	0.74	1.58 ± 0.09
0.02	0.36	0.26	2.15	0.74	1.68 ± 0.06
0.04	0.38	0.22	2.20	0.78	1.80 ± 0.08
0.06	0.39	0.21	2.34	0.79	1.93 ± 0.10
0.1	0.39	0.19	2.52	0.81	2.11 ± 0.09
0.15	0.38	0.16	2.70	0.84	2.33 ± 0.10
0.2	0.46	0.19	2.92	0.81	2.45 ± 0.08
0.25	0.40	0.15	2.90	0.85	2.52 ± 0.09
0.3	0.42	0.15	2.95	0.85	2.57 ± 0.06
0.4	0.44	0.17	2.97	0.83	2.54 ± 0.08
0.5	0.40	0.15	2.93	0.85	2.55 ± 0.10

the P105−CTAB system. This result clearly indicates that a relatively large number of CTAB molecules are required to pull the probe molecules from the micellar surface to its interior in the case of the F88 micelle, as compared to that in P105 micelle. Such a limiting value for P123−CTAC micellar system (corona thickness ~6 Å[41]) was found earlier to be ~0.15.[35] To understand the reason behind such variations in the limiting surfactant concentrations for different pluronics, a correlation plot between the limiting CTAB concentration and the thickness of the corona region of the micelles is shown in Figure 6. It is seen from this figure that the limiting surfactant concentration and the corona thickness follow a nice linear correlation. These

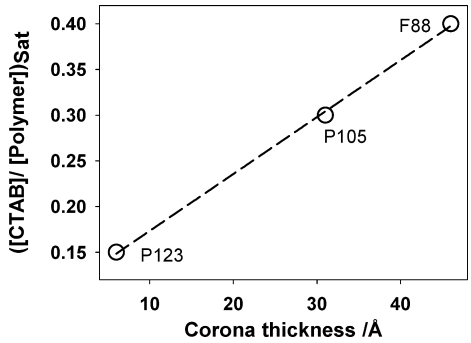

Figure 6. Linear correlation between the limiting value of the surfactant/polymer molar ratio and the thickness of the corona region of the block copolymer.

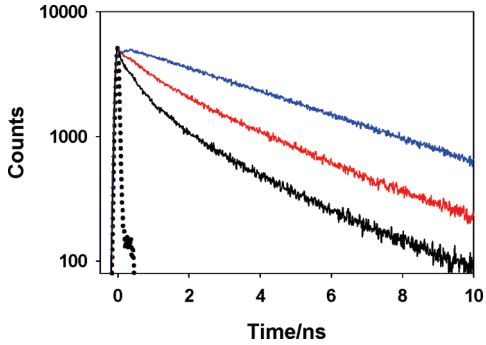

Figure 7. Transient fluorescence decays for C343 in a P105 micellar system at different emission wavelengths: (black) 440 nm, (red) 470 nm and (blue) 600 nm. The instrument response function (IRF) is shown by the dotted line.

results clearly indicate that as we increase the thickness of the corona region, the electrostatic attraction between the probe at the micellar surface and the positively charged layer inside the micelle will be relatively weaker. Because of this, a relatively higher charge density and, consequently, a larger CTAB concentration are required to pull the anionic C343 from the surface to the interior of the micelle.

3B.2. Dynamic Stokes' Shift Measurements. If the movement of the probe from the micellar surface to its interior with the addition of CTAB in the pluronic micelles is responsible for the observed changes in the reorientation time, then it would be expected that the water structure around the probe would also change simultaneously. It is expected that the probe when residing at the micellar surface would be surrounded by much more labile water, as compared to that when it is moved inside the corona region, where the extent of hydration is much less as compared to that at the micellar surface. This change in the hydration nature around the probe is expected to change the observed dynamic Stokes' shift due to the addition of CTAB to the micellar solution. To look into this aspect, detailed dynamic Stokes' shift measurements were carried out for the C343 dye in a P105 micellar solution at different CTAB concentrations. For this purpose, fluorescence transients were recorded at 10 nm intervals covering the full emission spectrum of the dye. All these fluorescence transients were fitted with a triexponential function using an iterative convolution and compare technique.[56] Time-resolved emission spectra (TRES) were then constructed following the method proposed by Maroncelli and Fleming.[57]

Figure 7 shows the fluorescence transients for C343 in a P105 micellar solution at different emission wavelengths. It is evident from this figure that emission at the blue edge of the spectrum shows a relatively faster decay component, whereas that at the red edge of the emission spectrum shows a slow growth, followed by longer decay components. These wavelength-dependent decay characteristics typically indicate the presence of a solvent relaxation process in the present system within the experimental time window. To understand this phenomena in detail, TRES were constructed and are shown in Figure 8A. It is evident from the TRES that there is a small red shift in the

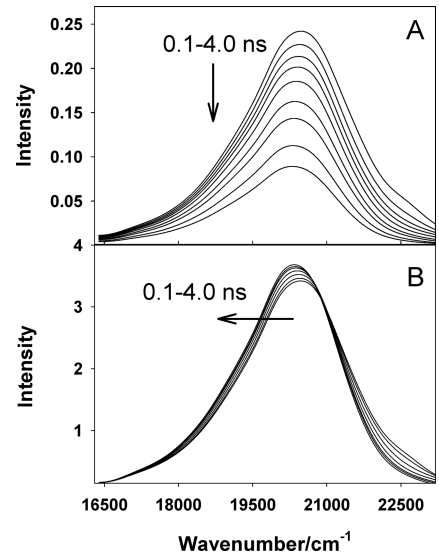

Figure 8. (A) Time-resolved emission spectra and (B) time-resolved area normalized emission spectra for C343 in a P105 micellar solution.

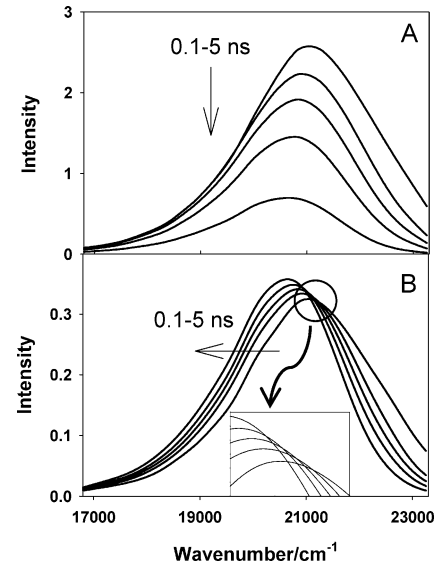

Figure 9. (A) Time-resolved emission spectra and (B) time-resolved area normalized emission spectra for C343 in a P105 micellar solution at a CTAB/P105 molar ratio of 0.4.

TABLE 4: Dynamic Stokes' Shift of C343 in P105 Micelle at Different CTAB Concentrations

	dynamic Stokes' shift		
[CTAB]/[P105]	$\Delta\omega_s^{total}/cm^{-1}$	$\Delta\omega_s^{obs}/cm^{-1}$	$\Delta\omega_s^{\%obs}$
0.00	2423	378	15.6
0.10	2255	485	21.5
0.15	2170	525	24.2
0.20	2084	550	26.4
0.30	2065	588	28.5
0.40	2041	592	29.0
0.50	2035	605	29.7

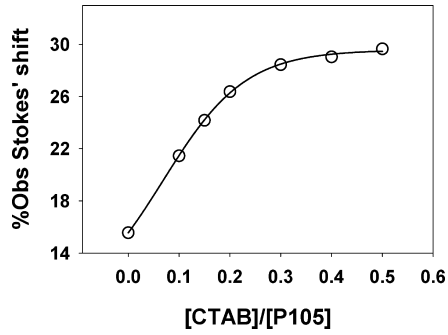

Figure 10. Variation in the percentage of Stokes' shift observed for the C343 dye in a P105 micellar solution vs the CTAB/P105 molar ratio.

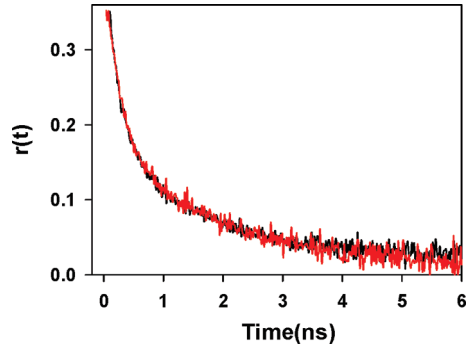

Figure 11. The anisotropy decay for C343 in P105−SDS supramolecular assemblies at different SDS/P105 molar ratios: (red) 0 and (black) 0.3.

emission spectra with time, along with a concomitant decrease in the emission intensity. To better understand the dynamic Stokes' shift, emission spectra were plotted after normalizing the area under each spectrum. The time-resolved area normalized emission spectra (TRANES)[58,59] for C343 in the P105 micellar solution are shown in Figure 8B. Note from Figure 8B that there is a small but definite red shift in the emission spectrum with time. In addition, note that there is an isoemissive point in TRANES. The appearance of an isoemissive point in TRANES is an indication of the presence of two emissive species in the present system.[58,59] The presence of two types of emissive species might be due to the distribution of the probe between the micellar and aqueous phases. As mentioned earlier, the probe C343 is present in its anionic form in the present experimental condition. Thus, there is a possibility that a small fraction of the dye may also be present in the bulk water phase, although a major fraction is expected to be associated with the micellar phase. Such a distribution of the C343 dye between the bulk water and the micellar phase has also been observed in other pluronic micelles[28,29] and in AOT reverse micelles.[32,36,37,60]

The TRES and TRANES for C343 in a P105 micellar system were also constructed in the presence of different CTAB concentrations. Figure 9A, B shows the TRES and TRANES, respectively, for the C343 dye in a P105−CTAB mixed micellar system at a CTAB/P105 molar ratio of 0.4. As in the P105 micelle, a dynamic Stokes' shift is also observed in the P105−CTAB mixed micellar system. However, the dynamic Stokes' shift observed for the mixed micellar system is found to be relatively larger, as compared to that in P105 micellar system. However, unlike in the P105 micellar system, no isoemissive point in the TRANES is observed in the presence of CTAB. The absence of any isoemissive point indicates that in the P105−CTAB mixed micellar system, only one emissive species is present. This result clearly indicates that due to the formation of a supramolecular assembly between the P105 micelle and the CTAB surfactant, all the probe molecules become associated with the micellar phase.

As mentioned above, the amount of dynamics Stokes' shift observed for the C343 dye in a P105 micellar system increases with an increase in the CTAB concentration. It is expected that due to the limited time resolution of the present experimental setup, a considerable amount of the dynamic Stokes' shift will remain unobserved. To estimate the percentage of dynamic Stokes' shift observed in the present system, we have calculated the expected total dynamic Stokes' shift following the method proposed by Fee and Maroncelli.[61] Thus, the total expected dynamics Stokes' shift was calculated after measuring the absorption and emission spectra of C343 in a nonpolar solvent (cyclohexane) and in micellar media using the following equation,[61]

$$\Delta\omega_s^{total} = [\omega_{abs}^{m} - \omega_{em}^{m}] - [\omega_{abs}^{CH} - \omega_{em}^{CH}] \qquad (9)$$

where ω_{abs}^{m} and ω_{abs}^{CH} are the absorption frequencies and ω_{em}^{m} and ω_{em}^{CH} are the emission frequencies of C343 dye in the micellar solution and in cyclohexane, respectively. Thus, the total expected dynamic Stokes' shift ($\Delta\omega_s^{total}$) and the observed dynamic Stokes' shift ($\Delta\omega_s^{obs}$) for C343 dye in the P105 micellar solution at different CTAB concentrations is presented in Table 4. The percentage of total dynamic Stokes' shift observed ($\Delta\omega_s^{\%obs}$) in these micellar systems is also presented in Table 4. The variation in the percentage of dynamic Stokes' shift

SCHEME 2: Schematic Representation of the Gradual Changes in the Location of an Anionic Solute with the Addition of a Cationic Surfactant in a Pluronic Micelle

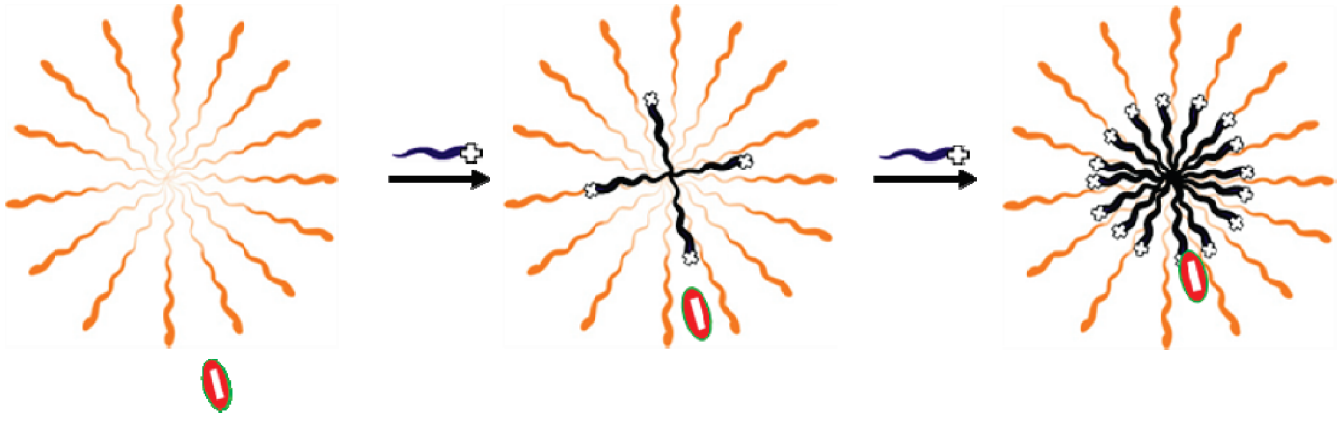

observed ($\Delta\omega_s^{\%obs}$) with the CTAB concentration is shown in Figure 10. It is evident from Figure 10 that as the concentration of the CTAB increases, the percentage of the dynamic Stokes' shift also increases and reaches a saturation value at a CTAB/P105 molar ratio of ∼0.3.

The observed changes in the dynamic Stokes' shift for C343 in a P105−CTAB mixed micellar system can be explained on the basis of the movement of the probe from the micellar surface to its interior due to the formation of a supramolecular assembly between the P105 micelle and the CTAB surfactant. In the absence of CTAB, the C343 dye resides on the micellar surface, where it is surrounded by restricted water molecules entrapped in the micellar phase and is also partially exposed to the bulk water. Due to very fast solvent relaxation of the bulk solvent (<1 ps[62,63]), large part of the dynamic Stokes' shift could not be observed with the limited time resolution of the present instrumental setup. Thus, only ∼15% of the total expected Stokes' shift is observed for C343 in the P105 micellar system. However, with the increase in the CTAB concentration, due to the formation of supramolecular assembly, the probe will experience an electrostatic attraction toward the interior of the micelle. As the probes moves toward the core−corona interface of the micelles, it is moving away from the bulk water. Thus, on addition of CTAB to the P105 micelle, the probe gradually feels less response from the bulk water and more response from the entrapped water inside the micelle, which is more restricted than that of the bulk water. Thus, due to the slow response of the entrapped water in the micelles, as the CTAB concentration increases, we gradually observe a more dynamic Stokes' shift. The movement of the probe from the micellar surface to its interior on addition of CTAB is also supported by the fact that the total Stokes' shift expected ($\Delta\omega_s^{total}$) also decreases with the increase in the CTAB concentration. This result clearly indicates that with an increase in the CTAB concentration, the probe migrates from a relatively higher polarity region to a relatively lower polarity region. The present dynamic Stokes' shift results are also in agreement with the results obtained from the time-resolved fluorescence anisotropy measurements and confirm the movement of the probe from the micellar surface to its interior on addition of CTAB to the P105 micellar solution.

To further understand the effect of repulsive electrostatic force on the location of the probe, we have also carried out time-resolved anisotropy measurements in the P105−SDS micellar system. Figure 11 shows the temporal anisotropy decay profile for C343 in a P105−SDS system at two different SDS concentrations. It is clearly indicated from Figure 11 that similar to the R101 probe in the F88−CTAB mixed micellar system discussed earlier, there is no change in the anisotropy decay profile for the C343 dye in the P105 micelle due to the addition of anionic surfactant, SDS. It is thus indicated that the anionic surfactant does not cause any movement of the anionic probe C343 in the P105−SDS supramolecular assembly. A similar observation has also been made in the F88−SDS micellar system.

4. Conclusions

In conclusion, the position of a suitable anionic probe in a pluronic micellar phase can be changed by adding a positively charged cosurfactant, CTAB. It is indicated from SANS studies that the addition of CTAB to a pluronic micellar solution results in the formation of supramolecular assemblies in which the hydrocarbon chain of the CTAB molecule resides in the core of the pluronic micelle and the headgroup of CTAB resides at the core−corona interface. The positively charged layer thus formed in the mixed micelles pulls the anionic probe from the micellar surface to its interior. Furthermore, it is shown that the concentration of the surfactant required to drag the probe molecule from the micellar surface to the core−corona interface vary linearly with the thickness of the corona region of the micelle. The change in the position of an anionic probe due to the addition of cationic surfactant in pluronic micelle can be schematically presented by Scheme 2.

The present study indicates that the effectiveness of a surfactant molecule to move a dissolved solute molecule from the surface to the interior of the micelle is largely determined by the thickness of the corona region, which in turn depends on the EO block size of the polymer used. From the present study, it can be inferred that by a proper selection of the polymer and the ionic surfactant, a suitably charged solute can be placed at different locations inside the mixed micelles by changing the concentration of the added surfactant. By controlling the position of the solute in the micellar system, it is thus possible to tune the physical as well as the chemical properties of the solute, which may have several applications, especially in the chemical synthesis and controlled drug release system.

Acknowledgment. We are thankful to Dr. G. B. Dutt for his useful suggestions during this work. We also thank Dr. T. Mukherjee, Director, Chemistry Group, BARC; and Dr. S. K. Sarkar, Head, Radiation & Photochemistry Division, BARC, for their constant encouragement and support during this work.

References and Notes

(1) Goddard, E. D. *J. Colloid Interface Sci.* **2002**, *256*, 228.
(2) Alexandridis, P.; Hatton, T. A. *Colloids Surf., A* **1995**, *96*, 1.
(3) Chu, B.; Zhou, Z. Physical chemistry of polyoxyalkylene block copolymer surfactants. In *Nonionic Surfactants*; Nace, V. M. , Ed.; Marcel Dekker: New York, 1996; Vol. 60; p 67.
(4) Alexandridis, P.; Holzwarth, J. F.; Hatton, T. A. *Macromolecules* **1994**, *27*, 2414.
(5) Wanka, G.; Hoffmann, H.; Ulbricht, W. *Macromolecules* **1994**, *27*, 4145.
(6) Nakashima, K.; Bahadur, P. *Adv. Colloid Interface Sci.* **2006**, *123−126*, 75.
(7) Bahadur, P.; Riess, G. *Tenside, Surfactants, Deterg.* **1991**, *28*, 173.
(8) Schmolka, I. R. *J. Am. Oil Chem. Soc.* **1980**, *59*, 322.
(9) Alakhov, V. Y.; Kabanov, A. V. *Expert Opin. Invest. Drugs* **1998**, *7*, 1453.
(10) Kabanov, A.; Zhu, J.; Alakhov, V. *Adv. Genet.* **2005**, *53*, 231.
(11) Nakashima, K.; Bahadur, P. *J. Controlled Release* **2002**, *82*, 189.
(12) Yokoyama, M. *Crit. Rev. Ther. Drug Carrier Syst.* **1992**, *9*, 213.
(13) Kataoka, K.; Harada, A.; Nagasaki, Y. *Adv. Drug Delivery Rev.* **2001**, *47*, 113.
(14) Wang, C. W.; Moffitt, M. G. *Langmuir* **2004**, *20*, 11784.
(15) Liu, T.; Burger, C.; Chu, B. *Prog. Polym. Sci.* **2003**, *28*, 5.
(16) Moffitt, M.; Vali, H.; Eisenberg, A. *Chem. Mater.* **1998**, *10*, 1021.
(17) Krishnamoorthy, S.; Pugin, R.; Brugger, J.; Heinzelmann, H.; Hoogerwerf, A. C.; Hinderling, C. *Langmuir* **2006**, *22*, 3450.
(18) Sakai, T.; Alexandridis, P. *Nanotechnology* **2005**, *16*, S344.
(19) Pancheri, E. J.; Mao, M. H. K. Comprising anionic surfactant polymeric nonionic surfactant and betaine surfactant U.S. Patent no. 5167872, 1992.
(20) Schaferf, R. Use of pluronic surfactant to enhance the cleaning effect of pancreatin on contact lenses. U.S. Patent no. 5672575, 1997.
(21) Jansson, J.; Schillen, K.; Nilsson, M.; Soderman, O.; Fritz, G.; Bergmann, A.; Glatter, O. *J. Phys. Chem. B* **2005**, *109*, 7073.
(22) Jansson, J.; Schillen, K.; Olofsson, G.; da Silva, R. C.; Loh, W. *J. Phys. Chem. B* **2004**, *108*, 82.
(23) Ganguly, R.; Aswal, V. K.; Hassan, P. A.; Gopalakrishnan, I. K.; Kulshreshth, S. K. *J. Phys. Chem. B* **2006**, *110*, 9843.
(24) Ganguly, R.; Aswal, V. K.; Hassan, P. A.; Gopalakrishnan, I. K.; Yakhmi, J. V. *J. Phys. Chem. B* **2005**, *109*, 5653.
(25) Mali, K. S.; Dutt, G. B.; Mukherjee, T. *J. Phys. Chem. B* **2007**, *111*, 5878.
(26) Lackowicz, J. R. *Principles of Fluorescence Spectroscopy*, 3rd ed.; Springer: New York, 2006.
(27) Aswal, V. K.; Goyal, P. S. *Curr. Sci.* **2000**, *79*, 947.

(28) Grant, C. D.; DeRitter, M. R.; Steege, K. E.; Fadeeva, T. A.; Castner, E. W. *Langmuir* **2005**, *21*, 1745.
(29) Grant, C. D.; Steege, K. E.; Bunagan, M. R.; Castner, E. W. *J. Phys. Chem. B* **2005**, *109*, 22273.
(30) Verma, P.; Nath, S.; Singh, P. K.; Kumbhakar, M.; Pal, H. *J. Phys. Chem. B* **2008**, *112*, 6363.
(31) Ma, J.; Guo, C.; Tang, Y.; Xiang, J.; Chen, S.; Wang, J.; Liu, H. *J. Colloid Interface Sci.* **2007**, *312*, 390.
(32) Riter, R. E.; Undiks, E. P.; Levinger, N. E. *J. Am. Chem. Soc.* **1998**, *120*, 6062.
(33) Kalyanasundaram, K. *Photochemistry in Microheterogeneous Systems*; Academic Press, Inc.: Orlando, 1987.
(34) Singh, P. K.; Kumbhakar, M.; Pal, H.; Nath, S. *J. Phys. Chem. B* **2008**, *112*, 7771.
(35) Singh, P. K.; Satpati, A. K.; Kumbhakar, M.; Pal, H.; Nath, S. *J. Phys. Chem. B* **2008**, *112*, 11447.
(36) Riter, R. E.; Kimmel, J. R.; Undiks, E. P.; Levinger, N. E. *J. Phys. Chem. B* **1997**, *101*, 8292.
(37) Riter, R. E.; Willard, D. M.; Levinger, N. E. *J. Phys. Chem. B* **1998**, *102*, 2705.
(38) Sen, P.; Ghosh, S.; Sahu, K.; Mondal, S. K.; Roy, D.; Bhattacharyya, K. *J. Chem. Phys.* **2006**, *124*, 204905.
(39) Ghosh, S.; Adhikari, A.; Mandal, U.; Dey, S.; Bhattacharyya, K. *J. Phys. Chem. C* **2007**, *111*, 8775.
(40) Kumbhakar, M.; Ganguly, R. *J. Phys. Chem. B* **2007**, *111*, 3935.
(41) Kumbhakar, M.; Geol, T.; Nath, S.; Mukherjee, T.; Pal, H. *J. Phys. Chem. B* **2006**, *110*, 25646.
(42) Kumbhakar, M.; Nath, S.; Mukherjee, T.; Pal, H. *J. Chem. Phys.* **2004**, *121*, 6026.
(43) Quitevis, E. L.; Marcus, A. H.; Fayer, M. D. *J. Phys. Chem.* **1993**, *97*, 5762.
(44) Chen, S. H.; Lin, T. L. Colloidal solutions. *In Methods of Experimental Physics: Neutron Scattering*; Price, D. L., Skold, K. , Eds.; Academic Press: New York, 1987; Vol. 23B; pp 489.
(45) Pedersen, J. S. *J. Appl. Crystallogr.* **2000**, *33*, 637.
(46) Pedersen, J. S.; Gerstenberg, C. *Macromolecules* **1996**, *29*, 1363.
(47) Percus, J. K.; Yevick, G. J. *Phys. Rev.* **1958**, *110*, 1.
(48) Mortensen, K.; Pederson, J. S. *Macromolecules* **1993**, *26*, 805.
(49) Ashcroft, N. W.; Leckner, J. *Phys. Rev.* **1966**, *145*, 83.
(50) Kinnig, D. J.; Thomas, E. L. *Macromolecules* **1984**, *17*, 1712.
(51) Jain, N. J.; Aswal, V. K.; Goyal, P. S.; Bahadur, P. *J. Phys. Chem. B* **1998**, *102*, 8452.
(52) Aswal, V. K.; Kohlbrecher, J. *Chem. Phys. Lett.* **2006**, *425*, 118.
(53) Almgren, M.; Stam, J. V.; Lindblad, C.; Li, P.; Stilbs, P.; Bahadur, P. *J. Phys. Chem.* **1991**, *95*, 5677.
(54) Mali, K. S.; Dutt, G. B.; Mukherjee, T. *J. Chem. Phys.* **2007**, *127*, 1549041.
(55) Yang, L.; Alexandridis, P. *Langmuir* **2000**, *16*, 4819.
(56) O'Connor, D. V.; Phillips, D. *Time Correlatated Single Photon Counting*; Academic: New York, 1984.
(57) Maroncelli, M.; Fleming, G. R. *J. Chem. Phys.* **1987**, *86*, 6221.
(58) Koti, A. S. R.; Krishna, M. M. G.; Periasamy, N. *J. Phys. Chem. A* **2001**, *105*, 1767.
(59) Koti, A. S. R.; Periasamy, N. *J. Chem. Phys.* **2001**, *115*, 7094.
(60) Willard, D. M.; Riter, R. E.; Levinger, N. E. *J. Am. Chem. Soc.* **1998**, *120*, 4151.
(61) Fee, R. S.; Maroncelli, M. *Chem. Phys.* **1994**, *183*, 235.
(62) Fecko, C. J.; Eaves, J. D.; Loparo, J. J.; Tokmakoff, A.; Geissler, P. L. *Science* **2003**, *301*, 1698.
(63) Jimenez, R.; Fleming, G. R.; Kumar, P. V.; Maroncelli, M. *Nature* **1994**, *369*, 471.
(64) Mortensen, K. *Polym. Adv. Technol.* **2001**, *12*, 2.

JP909333Q